2021

CT-guided versus MR-guided radiotherapy: Impact on gastrointestinal sparing in adrenal stereotactic body radiotherapy

Rupesh Kotecha
Baptist Health Medical Group; Miami Cancer Institute, rupeshk@baptisthealth.net

Martin Tom
Baptist Health Medical Group; Miami Cancer Institute, MartinTo@baptisthealth.net

Michael Chuong
Baptist Health Medical Group; Miami Cancer Institute, michaelchu@baptisthealth.net

Jessika Contreras
Baptist Health Medical Group; Miami Cancer Institute, jessikaac@baptisthealth.net

Tino Romaguera
Miami Cancer Institute, AntinogenesR@baptisthealth.net

See next page for additional authors

Citation

Radiotherapy and Oncology (2021) [Epub ahead of print] Published online: November 26

Authors

Rupesh Kotecha, Martin Tom, Michael Chuong, Jessika Contreras, Tino Romaguera, Diane Alvarez, James McCulloch, Robert Herrera, Jairo Mercado, Minesh Mehta, Alonso Gutierrez, Kathryn Mittauer, Rene Hernandez, and Lori Rodriguez

Radiotherapy and Oncology 166 (2022) 101–109

Contents lists available at ScienceDirect

Radiotherapy and Oncology

journal homepage: www.thegreenjournal.com

Original Article

CT-guided versus MR-guided radiotherapy: Impact on gastrointestinal sparing in adrenal stereotactic body radiotherapy

Lori L. Rodriguez [a], Rupesh Kotecha [a,b], Martin C. Tom [a,b], Michael D. Chuong [a,b], Jessika A. Contreras [a,b], Tino Romaguera [a,b], Diane Alvarez [a,b], James McCulloch [a,b], Robert Herrera [a], Rene J. Hernandez [a], Jairo Mercado [a], Minesh P. Mehta [a,b], Alonso N. Gutierrez [a,b], Kathryn E. Mittauer [a,b,*]

[a] Department of Radiation Oncology, Miami Cancer Institute, Baptist Health South Florida; and [b] Herbert Wertheim College of Medicine, Florida International University, Miami, USA

ARTICLE INFO

Article history:
Received 8 June 2021
Received in revised form 18 November 2021
Accepted 21 November 2021
Available online 26 November 2021

Keywords:
MR-guided radiotherapy
Adrenal cancer
SBRT
Adaptive radiotherapy
Motion management

ABSTRACT

Background and purpose: To quantify the indication for adaptive, gated breath-hold (BH) MR-guided radiotherapy ($MRgRT_{BH}$) versus BH or free-breathing (FB) CT-based image-guided radiotherapy (CT-IGRT) for the ablative treatment of adrenal malignancies.

Materials and methods: Twenty adrenal patients underwent adaptive IMRT $MRgRT_{BH}$ to a median dose of 50 Gy/5 fractions. Each patient was replanned for VMAT CT-$IGRT_{BH}$ and CT-$IGRT_{FB}$ on a c-arm linac. Only CT-$IGRT_{FB}$ used an ITV, summed from GTVs of all phases of the 4DCT respiratory evaluation. All used the same 5 mm GTV/ITV to PTV expansion. Metrics evaluated included: target volume and coverage, conformality, mean ipsilateral kidney and 0.5 cc gastrointestinal organ-at-risk (OAR) doses ($D_{0.5cc}$). Adaptive dose for $MRgRT_{BH}$ and predicted dose (i.e., initial plan re-calculated on anatomy of the day) was performed for CT-$IGRT_{BH}$ and $MRgRT_{BH}$ to assess frequency of OAR violations and coverage reductions for each fraction.

Results: The more common VMAT CT-$IGRT_{FB}$, with its significantly larger target volumes, proved inferior to $MRgRT_{BH}$ in mean PTV and ITV/GTV coverage, as well as small bowel $D_{0.5cc}$. Conversely, VMAT CT-$IGRT_{BH}$ delivered a dosimetrically superior initial plan in terms of statistically significant ($p \leq 0.02$) improvements in target coverage, conformality and $D_{0.5cc}$ to the large bowel, duodenum and mean ipsilateral kidney compared to IMRT $MRgRT_{BH}$. However, non-adaptive CT-$IGRT_{BH}$ had a 71.8% frequency of predicted indications for adaptation and was 2.8 times more likely to experience a coverage reduction in PTV $D_{95\%}$ than predicted for $MRgRT_{BH}$.

Conclusion: Breath-hold VMAT radiotherapy provides superior target coverage and conformality over $MRgRT_{BH}$, but the ability of $MRgRT_{BH}$ to safely provide ablative doses to adrenal lesions near mobile luminal OAR through adaptation and direct, real-time motion tracking is unmatched.

Ablative stereotactic body radiotherapy (SBRT) has been demonstrated to be a promising treatment for unresectable adrenal metastases [1–3]. Additionally, a higher biologically effective dose (BED_{10}, α/β = 10) is associated with significant increases in local control and overall survival [1,4,5]. For BED_{10} values of 60 Gy, 80 Gy, and 100 Gy, a recent meta-analysis by Chen *et al.* predicted 2-year local control (LC) rates of 47.8%, 70.1%, and 85.6% and overall survival (OS) rates of 34.0%, 47.2% and 60.1% [1]. However, delivering ablative dose to the entirety of the target is often compromised by overlapping organs at risk (OAR) [6,7], which may be exacerbated by the larger target volume required to encompass the full motion envelope with respiration. Currently, the role of motion management on the resulting dose distribution for adrenal SBRT is unclear.

The same meta-analysis revealed that the most common method of respiratory motion management for adrenal SBRT is free breathing, internal target volume (ITV) contouring through four-dimensional computed tomography (4DCT) [1]. De Kuijer et al., in a limited series of 11 patients, quantified the motion of adrenal glands between breath hold (BH) and free breathing (FB) on 4DCT and found an overall reduction in the target volume favoring the use of BH [8]. A clinical extrapolation of this premise is that the reduction of target volume may enable dose escalation to a large volume of the tumor for adrenal SBRT, which may potentially improve long-term local control [1,4].

Magnetic resonance guided radiotherapy (MRgRT), using the MRIdian Linac (ViewRay Inc., Oakwood, OH, USA), enables breath hold motion management through direct real-time soft tissue

* Corresponding author at: Department of Radiation Oncology, Miami Cancer Institute, Baptist Health South Florida, 8900 N Kendall Dr., Miami, FL 33176, USA.
E-mail address: kathrynm@baptisthealth.net (K.E. Mittauer).

https://doi.org/10.1016/j.radonc.2021.11.024
0167-8140/

tracking of the gross disease, without the need for surrogate anatomical tracking, implanted fiducials, tidal-volume spirometry, or external markers, as may be warranted in CT-based image-guided radiotherapy (IGRT) systems [9–11]. Consequently, the use of MRgRT with BH may be an effective strategy to minimize target volume and thereby reduce OAR dose, while maintaining or improving tumor coverage.

Additionally, MRgRT provides the ability to perform daily online adaptation [6,9,12]. Palacios et al. demonstrated that stereotactic MR-guided adaptive radiation therapy (SMART) for adrenal metastases allows target dose escalation and simultaneous gastrointestinal (GI) OAR sparing [6]. While their work quantified the dosimetric indications for adaptation for adrenal metastases, it did not quantify the dosimetric differences between MR-guided real-time breath-hold tracking compared to the standard CT-based free breathing strategies. Reports of other abdominal and thoracic sites have demonstrated the dosimetric advantages of a reduction in dose to the surrounding normal tissues in BH compared to FB plans [8,13–15].

The purpose of this study is to quantitatively evaluate the indication for mid-inspiration breath-hold MR-guided radiotherapy compared to the standard treatment technique of CT-based image guided radiotherapy in the stereotactic ablation of adrenal malignancies. To the best of our knowledge, this is the first study to quantify both the indication for adaptation and the differences between breath-hold MRgRT and free-breathing/breath-hold CT-IGRT for adrenal lesions, using previously obtained clinical imaging.

Materials and methods

Study overview

Twenty patients, at a single institution, were treated with mid-inspiration BH MR-guided radiotherapy to a median dose of 50 Gy in 5 fractions for stereotactic ablation of adrenal metastases. A summary of patient characteristics is provided in Table A1. Most patients had adrenal metastases resulting from adenocarcinoma of the lung (n = 12). The patients were evenly divided by sex, with a slightly larger number of left adrenal lesions (n = 11) than right (n = 9).

An overview of the study methods is presented in Fig. 1. In this institutional review board (IRB) approved study, there are three arms: breath-hold step-and-shoot IMRT MR-guided radiotherapy ($MRgRT_{BH}$), breath-hold VMAT CT-based image-guided radiotherapy ($CT\text{-}IGRT_{BH}$), and free-breathing VMAT CT-based image-guided radiotherapy ($CT\text{-}IGRT_{FB}$). The indication for FB ($CT\text{-}IGRT_{FB}$) versus gated BH delivery ($MRgRT_{BH}$) was evaluated through the dosimetric differences in target volume, gastrointestinal luminal organs, and ipsilateral kidney. To isolate the impact of FB versus BH in the change from IMRT to VMAT, we assessed the initial $CT\text{-}IGRT_{BH}$ plans compared to $MRgRT_{BH}$. Lastly, we investigated the effects of daily MR adaptation versus non-adaptive $CT\text{-}IGRT_{BH}$ by registering the initial $CT\text{-}IGRT_{BH}$ plans (approximated on the simulation MRI) to the daily setup MR scans to quantify the predicted dose for the $CT\text{-}IGRT_{BH}$ arm.

$MRgRT_{BH}$ simulation and segmentation

Patient simulation was performed in the supine position with the ipsilateral arm raised over the head, except for a few instances where patient tolerance dictated that both arms be down at their sides. No immobilization was required for simulation due to the use of real-time intrafraction MR tracking. A planning 0.35T, 3D mid-inspiration breath hold (BH), true fast imaging with steady-state free precession (TrueFISP) MR scan was acquired on the MRIdian Linac followed by a BH CT for electron density information and a 4DCT for respiratory evaluation on a SOMATOM Definition Edge (Siemens Healthcare, Forchheim, Germany).

Segmentation of the gross tumor volume (GTV) was performed by a disease site-specialized radiation oncologist on the BH MR planning scan. In all cases, the planning target volume (PTV) was defined by an isotropic 5 mm expansion of the GTV. Because the patients were to receive gated BH delivery, no ITV was defined for the MRgRT plan. OAR segmentation included large and small bowel, stomach, duodenum, liver, spinal cord and both kidneys. All contours were peer-reviewed prior to treatment.

$MRgRT_{BH}$ planning and treatment

Patients were prescribed a median dose of 50 Gy (n = 6 at 40 Gy, n = 14 at 50 Gy) in 5 fractions to at least 99% of the GTV and 95% of the PTV. The median BED_{10} value was 100 Gy (72 Gy for the 40 Gy in 5 fractions treatments). A standardized institutional treatment planning approach was used for all $MRgRT_{BH}$ plans and will be briefly summarized here. Full target coverage was not always possible while still respecting OAR constraints, so a 3 mm margin was generated around the GI OARs to create a planning organ-at-risk volume (PRV_{GI}). Optimized target volumes (PTV_{opt} and GTV_{opt}) were created from the physician's delineated PTV and GTV and truncated at the edges of this PRV_{GI} during planning. PTV_{opt} and GTV_{opt} were optimized to the prescription dose, while the overlapping OARs were constrained to their maximum allowed limits according to the treatment planning directive. Plan quality was driven until either full PTV and GTV coverage was achieved or until maximum tolerance was reached for a single OAR. A 3 to 5 mm contraction of the GTV_{opt} was driven to a minimum of 120% of the prescription dose, with a maximum point dose of 135–140%, to provide an ablative hotspot to the center of the adrenal tumor without increasing the dose gradient near the OARs. In order to control low dose conformality, the 50% isodose volume was constrained to fall within the confines of a 1 cm thick shell, created from isotropic 2 and 3 cm expansions of the PTV_{opt}.

Table A2 (Appendix) provides an overview of the OAR constraints used for the patients included in this study. While the majority of patients had both a maximum dose to 0.5 cc ($D_{0.5cc}$) and maximum dose to 0.03 cc ($D_{0.03cc}$) for the bowel OARs, few patients had $D_{0.03cc}$ constraints for the other GI OARs. Of note, a range of OAR constraints are shown in Table A2, due to the enrollment of a subset of patients on clinical trials with differing OARs constraints.

Treatment plans were step-and-shoot IMRT with beam arrangements generally spaced unilaterally (i.e., 200 degrees, n = 12 plans) around the target with avoidance sectors for entrance beams within 2 cm of patient arms or couch edges. The remaining patients (n = 8 plans) were treated approximately isotropically with similar avoidance structures. The number of beams ranged from 12 to 21 (median 17). The number of segments was between 27 and 77 (median 46). Electron density for the calculation of dose on the MR scan was provided by deformable registration of the BH CT to the BH MR scan [16]. Manual electron density corrections were included when necessary. Dose was calculated with a Monte Carlo algorithm to an isotropic grid resolution of 2 mm × 2 mm × 2 mm, including magnetic field corrections.

All patients underwent daily online adaptation. For daily MR guidance, patient localization was achieved through alignment of the GTV on the daily fractional 3D MR setup scan. Targets were rigidly copied from the MR simulation scan to the MR of the day, while OARs were deformably registered to the MR of the day frame of reference. The GTV was manually edited to account for target deformations and the PTV was manually re-expanded. OARs were manually edited within 2 cm axially and 3 cm superior-inferior of the PTV surface. The initial treatment plan was recalculated on

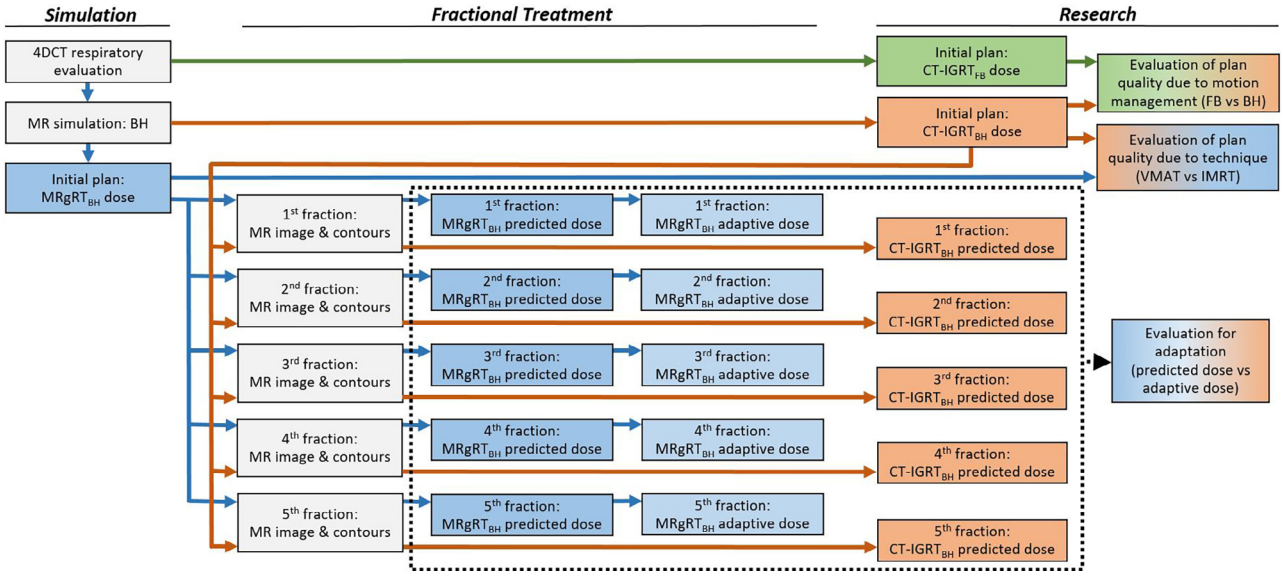

Fig. 1. Overview of study methods.

the anatomy of the day (i.e., predicted dose) to evaluate the indication for adaptation, based on target coverage and/or OAR constraints as outlined by the treatment planning directive. If this predicted dose failed to meet the prescribed metrics, then the plan was re-optimized and normalized with the adaptive plan used for patient treatment.

Treatment delivery was performed using real-time tracking for all patients. The tracking region of interest (ROI) was deformed to the real-time sagittal cine plane at 4 frames per second. A 3 mm isotropic expansion from the tracking ROI was used to delineate the boundary limit of excursion. Gated delivered was performed such that the beam turned off if greater than 5% of the tracking ROI was outside this boundary.

In addition to statistics of beam geometry and modulation, the treatment time was also recorded for all patients included in this study. Treatment time was calculated from the timestamp of the patient entering the vault to the completion of radiation delivery for MRgRT$_{BH}$ fractions.

CT-IGRT$_{FB}$ simulation and segmentation

The CT-IGRT$_{FB}$ plans were calculated on the average intensity projection (AIP) CT constructed from the 4DCT performed during MRgRT$_{BH}$ respiratory evaluation. OAR segmentation was also done on the AIP-CT by a board-certified medical physicist, with visual reference to the corresponding OARs done for MRgRT$_{BH}$. A disease-site specialized radiation oncologist reviewed, edited, and approved all normal OAR segmentation. The same radiation oncologist segmented the GTV on each phase of the 4DCT, which was then summed to define the ITV. A uniform 5 mm expansion from the ITV was used to create the PTV, equivalent to the PTV expansion used on MRgRT$_{BH}$. The ITV and the OAR segmentation were each peer-reviewed by a second disease-site specialized radiation oncologist.

CT-IGRT$_{FB}$ planning

Each patient was retrospectively replanned to a 3-arc, volumetric-modulated arc therapy (VMAT) CT-IGRT$_{FB}$ treatment on a c-arm linac with high-definition multi-leaf collimators. Treatment planning was performed in Eclipse Acuros version 15.6.06 (Varian Medical Systems, Palo Alto, CA, USA) on an isotropic 1.25 mm × 1.25 mm × 1.25 mm calculation grid. Hemispherical (180°) ipsilateral arcs proved insufficient to provide target coverage to the medial edges of the PTV, so most patients were treated by beams that extended 45° over the anterior thorax (i.e., 225°). Two of the patients, with very large PTVs (volume > 150 cc), were treated to larger angles. Because some patients had both arms at their sides during MRgRT$_{BH}$ simulation, avoidance sectors were used to prevent entrance doses to their limbs. The net active arc lengths for the CT-IGRT$_{FB}$ treatments ranged from 166° to 319° (median 224°).

The CT-IGRT$_{FB}$ ITV and PTV were planned to the same 40–50 Gy doses with the same 99% and 95% minimum coverage requirements as the corresponding MRgRT$_{BH}$ GTV and PTV, with the same stipulation that the OAR constraints had to be met. The targets were truncated to an ITV$_{opt}$ and PTV$_{opt}$ if overlapped with the PRV$_{GI}$. To mirror the MRgRT$_{BH}$ technique, CT-IGRT$_{FB}$ optimization was performed until either full PTV and ITV coverage was achieved or until maximum tolerance was reached for a single OAR. A 3–5 mm contraction of the ITV$_{opt}$ was driven to a minimum of 120% of the prescription dose, with a maximum point dose between 130% and 140%, so that hotspots would fall in the center of the adrenal tumor without excessive dose gradients near sensitive OARs. The 50% isodose volume was again constrained to fall within the limits of the 2–3 cm shell around the PTV, to ensure low dose conformality. Two disease-site specialized radiation oncologists approved each of the CT-IGRT$_{FB}$ plans which were never used in treatment. Because daily 4DCTs were not performed, the CT-IGRT$_{FB}$ arm could not be evaluated for the indication for adaptation.

For comparison to the MRgRT$_{BH}$, the treatment times for CT-IGRT were approximated. Since abdominal SBRT are triaged to MRgRT and are not generally treated on a c-arm linac, the median treatment time for the CT-IGRT plans was approximated by using the times for lung SBRT treatments as a surrogate for adrenal metastases. Lung SBRT treatment times from a single c-arm linac were collected from the past 12 months.

CT-IGRT$_{BH}$ simulation and segmentation

Daily CTs of patients treated on the MR-linac were not acquired, therefore the CT-IGRT$_{BH}$ plans were calculated on the same initial and daily setup breath-hold MRIs used for MRgRT$_{BH}$ planning, with bulk density overrides. The simulation and fractional segmentation approved for MRgRT$_{BH}$ was used for the corresponding CT-IGRT$_{BH}$ plans.

CT-IGRT$_{BH}$ planning

To generate the CT-IGRT$_{BH}$ initial plan, the MRI and structure set for each patient's initial MRgRT$_{BH}$ plan were imported into Eclipse and rigidly registered to the GTV, by a board certified medical physicist, to the previously calculated CT-IGRT$_{FB}$ plan. The MR and structure set were assigned as the primary to enable the previously-used optimization values of the CT-IGRT$_{FB}$ plan as a starting point for the CT-IGRT$_{BH}$ plan generation. The bulk densities corresponding to the MRgRT$_{BH}$ plans were used in Eclipse. Bulk densities included tissue (1 g/cc), air (0.0012 g/cc), and for a subset of patients bone (1.12 g/cc) and lung (0.260 g/cc). The plans were then re-optimized to meet all of the original prescription constraints and normalized to either full target coverage or until maximum tolerance was reached for a single OAR.

The daily setup BH MRIs for the five treatment fractions were imported into Eclipse along with the structure sets that were generated and approved during on-table adaptation. The fractional MRIs were registered based on GTV alignment to the initial CT-IGRT$_{BH}$ plans just as described. After assigning bulk densities consistent with the initial CT-IGRT$_{BH}$ plans, the initial plan was recalculated, without re-optimization, on the anatomy of the day yielding the predicted CT-IGRT$_{BH}$ dose for targets and OARs.

Indication for adaptation CT-IGRT$_{BH}$ and MRgRT$_{BH}$

OAR and target coverage metrics were compared between the adaptive MRgRT$_{BH}$ dose, predicted MRgRT$_{BH}$ dose, and predicted CT-IGRT$_{BH}$ dose. Daily fractions that would have violated the OAR constraints or delivered a reduction in target coverage (to the relative D95%/D_{Rx} dose to the PTV or GTV), were counted and the frequency of violations calculated as a percent of constrained fractions. An exception was made for the mean ipsilateral kidney. The ipsilateral kidney was intentionally violated during adaptation on some fractions at the physician's direction to prioritize target coverage. Therefore, an ipsilateral kidney violation was only counted if it exceeded the dose approved and delivered by the corresponding adaptive MRgRT$_{BH}$ treatment.

Statistical analysis

Differences in target volume metrics between the initial MRgRT$_{BH}$ plan and both the CT-IGRT$_{BH}$ and CT-IGRT$_{FB}$ plans were evaluated for target coverage (TC) (PTV $V_{100\%}/V_{PTV}$ and GTV $V_{100\%}/V_{GTV}$), relative dose to 95%, 90%, 80% and mean PTV and GTV volumes (i.e., $D_{95\%}/D_{Rx}$, $D_{90\%}/D_{Rx}$, $D_{80\%}/D_{Rx}$, and D_{mean}/D_{Rx}), homogeneity index (HI) (PTV $D_{2\%}/D_{98\%}$), prescription isodose to target volume (PITV) ratio (i.e., volume of the 100% isodose line/V_{PTV}), low dose conformity (D_{2cm}) (i.e., maximum dose within 2 cm in any direction from the PTV), and gradient ($R_{50\%}$) (i.e., volume of the 50% isodose line/V_{PTV}). Additional metrics evaluated were the mean ipsilateral kidney dose and the doses to 0.5 cc ($D_{0.5cc}$) of the GI OARs: small bowel, large bowel, duodenum and stomach.

Statistical analysis was performed on Origin software (OriginLab, Northampton, Massachusetts, USA). A Wilcoxon signed-rank test for non-normal distributions was used to assess the statistical differences between MRgRT$_{BH}$ and CT-IGRT$_{BH}$ and between MRgRT$_{BH}$ and CT-IGRT$_{FB}$. Differences were not assessed between the CT-IGRT$_{FB}$ and CT-IGRT$_{BH}$ plans, as this has been previously reported in the literature. Because the distribution of metrics was skewed, median values are given with their interquartile (Q2-Q3) range (IQR). Statistically significant difference was taken as $p < 0.05$.

Results

The target volumes and dosimetric metrics for conformality, coverage, organs at risk, and degree of modulation across the 20 patients are displayed in Table 1 for initial MRgRT$_{BH}$ ($n = 20$ plans) versus CT-IGRT$_{BH}$ ($n = 20$ plans) and CT-IGRT$_{FB}$ ($n = 20$ plans). There was a statistically significant decrease ($p < 0.01$) in median PTV volumes for CT-IGRT$_{BH}$ at 48.9 cc (IQR: 33.1–79.0 cc) versus

Table 1
Comparison of median (and interquartile range) target volume, conformality, coverage, organ-at-risk dose and modulation between the initial plans for breath-hold MR-guided radiotherapy (MRgRT$_{BH}$) versus both breath-hold and free-breathing CT image-guided radiotherapy (CT-IGRT$_{BH}$ and CT-IGRT$_{FB}$).

	Metric	Metric unit	MRgRT$_{BH}$		CT-IGRT$_{BH}$		p value	CT-IGRT$_{FB}$		p value
Target	PTV volume	cc	53.6	(37.1–86.1)	48.9	(33.1–79.0)	$p < 0.01$	91.9	(45.0–135.4)	$p < 0.01$
	GTV or ITV volume	cc	24.6	(14.0–38.5)	21.2	(11.6–34.7)	$p < 0.01$	43.4	(16.6–69.2)	$p < 0.01$
Conformality	PITV	$V_{100\%\ Rx\ iso}/V_{PTV}$	1.03	(0.98–1.08)	1.03	(0.95–1.11)	NS	0.95	(0.92–1.02)	$p < 0.01$
	Homogeneity index	PTV at $D_{2\%}/D_{98\%}$	1.43	(1.29–2.02)	1.33	(1.25–1.50)	$p < 0.01$	1.67	(1.28–2.18)	NS
	$R_{50\%}$	$V_{50\%\ Rx\ iso}/V_{PTV}$	3.99	(3.58–4.28)	3.51	(3.13–3.90)	$p < 0.01$	3.22	(3.02–3.39)	$p < 0.01$
	Max D_{2cm}	% of D_{Rx} @ 2 cm from PTV	57.2	(52.2–60.8)	55.4	(53.1–56.4)	NS	57.4	(55.5–61.7)	NS
Coverage	PTV coverage	$V_{PTV\ at\ 100\%\ Rx}/V_{PTV}$	0.95	(0.88–0.95)	0.96	(0.92–0.99)	$p < 0.01$	0.93	(0.87–0.97)	NS
	GTV or ITV coverage	$V_{GTV\ at\ 100\%\ Rx}/V_{GTV}$	1.00	(0.97–1.00)	1.00	(1.00–1.00)	$p < 0.01$	1.00	(0.96–1.00)	NS
	PTV $D_{95\%}$	% of Rx	1.00	(0.83–1.00)	1.02	(0.97–1.07)	$p < 0.01$	0.98	(0.69–1.03)	NS
	PTV $D_{90\%}$	% of Rx	1.02	(0.97–1.03)	1.05	(1.02–1.11)	$p < 0.01$	1.02	(0.90–1.05)	NS
	PTV $D_{80\%}$	% of Rx	1.06	(1.05–1.08)	1.07	(1.06–1.13)	NS	1.06	(1.05–1.08)	NS
	PTV D_{mean}	% of Rx	1.13	(1.11–1.16)	1.12	(1.09–1.17)	NS	1.08	(1.07–1.13)	$p < 0.01$
	GTV or ITV $D_{95\%}$	% of Rx	1.08	(1.05–1.13)	1.07	(1.06–1.12)	NS	1.06	(1.03–1.10)	$p = 0.045$
	GTV or ITV $D_{90\%}$	% of Rx	1.10	(1.09–1.17)	1.08	(1.06–1.13)	NS	1.08	(1.04–1.11)	$p = 0.02$
	GTV or ITV $D_{80\%}$	% of Rx	1.14	(1.11–1.20)	1.09	(1.08–1.15)	NS	1.10	(1.06–1.13)	$p < 0.01$
	GTV or ITV D_{mean}	% of Rx	1.20	(1.15–1.23)	1.14	(1.12–1.19)	NS	1.12	(1.09–1.15)	$p < 0.01$
Organs at Risk	Large bowel $D_{0.5cc}$	Gy	18.4	(15.0–21.9)	15.4	(13.5–21.6)	p = 0.02	21.5	(15.6–24.5)	NS
	Small bowel $D_{0.5cc}$	Gy	13.9	(3.2–29.9)	6.4	(1.4–24.5)	NS	19.7	(9.3–31.9)	p = 0.04
	Duodenum $D_{0.5cc}$	Gy	18.2	(10.9–22.0)	14.4	(10.2–21.0)	p < 0.01	23.5	(6.5–30.6)	NS
	Stomach $D_{0.5cc}$	Gy	24.6	(18.4–33.4)	22.1	(13.7–32.8)	NS	24.0	(19.5–32.7)	NS
	Ipsilateral kidney D_{mean}	Gy	7.1	(5.3–9.5)	5.1	(3.1–8.0)	p < 0.01	7.5	(6.0–9.7)	NS
Modulation	Beams	number	17	(14–18)	3 arcs	-	3 arcs	-		
	Segments	segments or arc degrees	46	(40–57)	224°	(217-225°)	-	224°	(217-225°)	-
	Total treatment time (with full range)*	min	64	(30–128)	-	-	-	32	(22–72)	-

Note: Planning target volume (PTV), gross tumor volume (GTV), internal target volume (ITV), prescription isodose to target volume (PITV), homogeneity index (HI), gradient ($R_{50\%}$), low dose conformity (D_{2cm}), dose to at least 95% of volume ($D_{95\%}$), dose to at least 90% of volume ($D_{90\%}$), dose to at least 80% of volume ($D_{80\%}$), mean dose (D_{mean}), maximum dose to 0.5 cc of volume ($D_{0.5cc}$), second quartile (Q2), third quartile (Q3)

$MRgRT_{BH}$ at 53.6 cc (IQR: 37.1–86.1 cc). There was a statistically significant increase ($p < 0.01$) in median PTV volumes for CT-$IGRT_{FB}$ at 91.9 cc (IQR: 45.0–135.4 cc) over $MRgRT_{BH}$.

All target coverage metrics in Table 1 are expressed as dose relative to the prescribed dose, to account for the difference in prescriptions (i.e., 40 Gy vs 50 Gy). A statistically significant ($p < 0.01$) increase in PTV coverage was observed for CT-$IGRT_{BH}$ over $MRgRT_{BH}$ for $D_{90\%}$ (median 1.05 vs 1.02), $D_{95\%}$ (median 1.02 vs 1.00), and relative $V_{100\%}/V_{Rx}$ PTV TC (0.96 vs 0.95) and GTV TC (1.00 vs 1.00, where the IQR ranges were 1.00 - 1.00 vs 0.97 - 1.00). No difference was seen for PTV_{mean} or $D_{80\%}$, nor for GTV_{mean} or any other GTV metrics.

An increase in PTV coverage, though not statistically significant, was observed for $MRgRT_{BH}$ compared to CT-$IGRT_{FB}$ for $D_{95\%}$, and TC. No difference was seen for PTV $D_{90\%}$ and $D_{80\%}$. A statistical difference was observed for GTV versus ITV coverage at $D_{90\%}$ (median 1.10 vs 1.08), $D_{80\%}$ (1.14 vs 1.10), and D_{mean} (1.20 vs 1.12). The median of the mean relative PTV dose was also significantly higher at 1.13 for $MRgRT_{BH}$ versus 1.08 for CT-$IGRT_{FB}$.

For the BH plans, mean homogeneity and conformality indices for CT-$IGRT_{BH}$ versus $MRgRT_{BH}$ (Table 1) were 1.33 versus 1.43 for HI ($p < 0.01$), and 3.51 versus 3.99 for $R_{50\%}$ ($p < 0.01$), but not statistically different for PITV or maximum dose at 2 cm. While for the FB versus BH comparison, CT-$IGRT_{FB}$ and $MRgRT_{BH}$ values were 0.95 and 1.03 for PITV ($p < 0.01$), 3.22 and 3.99 for $R_{50\%}$ ($p < 0.01$), but not statistically different for HI or D_{2cm}.

The median $MRgRT_{BH}$ treatment time was 64 minutes (range: 30–28 minutes, $n = 95$ appointments). The scheduled $MRgRT_{BH}$ appointment duration was 90 minutes. The median treatment time for lung SBRT patients ($n = 66$ appointments) was 32 minutes (range: 22–72 minutes). All lung SBRT patients were FB with abdominal compression alone, i.e., no intra-fraction monitoring or gating. The scheduled CT-IGRT appointment was 60 minutes for first fraction and 40 minutes for subsequent fractions.

Fig. 2 displays boxplots of the mean, median and interquartile ranges of the OAR doses for $MRgRT_{BH}$, CT-$IGRT_{BH}$ and CT-$IGRT_{FB}$. The boxes span the interquartile range (IQR) from quartile 2 to 3, the median is shown as a horizontal line, and the mean as an "x." The whiskers represent 1.5 times the interquartile range, with outliers not displayed. The CT-$IGRT_{BH}$ plans show a clear improvement over the $MRgRT_{BH}$ plans in maximum dose to 0.5 cc of the large bowel (15.4 vs 18.4 Gy, $p = 0.02$), the duodenum (14.4 vs 18.2 Gy, $p < 0.01$) and the mean ipsilateral kidney (5.1 vs 7.1 Gy, $p < 0.01$). There were only marginal decreases in $D_{0.5cc}$ to the small bowel and the stomach. $MRgRT_{BH}$ exhibited a significant 42% reduction in $D_{0.5cc}$ ($p = 0.04$) to the small bowel compared to CT-$IGRT_{FB}$ (13.9 vs 19.7 Gy) and marginal reductions to the ipsilateral kidney, duodenum and large bowel.

A visual representation of the loss of low dose conformality was observed in Fig. 3 for the larger targets in CT-$IGRT_{FB}$ (Fig. 3C) compared to the $MRgRT_{BH}$ and CT-$IGRT_{BH}$ plans (Fig. 3A and 3B), though in the aggregate, D_{2cm} was statistically equivalent between the three treatment techniques. A reduction in the OAR-to-PTV proximity was observed in Fig. 3 with a greater increase in the volume of overlap between the PTV (cyan ROI) and small bowel (blue ROI) in CT-$IGRT_{FB}$ (Fig. 3F) compared to $MRgRT_{BH}$ and CT-$IGRT_{BH}$ plans (Fig. 3D and 3E). Note that the smaller GTVs for the BH plans do not extend into this axial slice, while the larger ITV is shown on the CT-$IGRT_{FB}$ plan (green ROI).

Table 2 displays the indication for adaptation evaluated from the CT-$IGRT_{BH}$ ($n = 95$ fractions) and $MRgRT_{BH}$ ($n = 95$ fractions) predicted dose (i.e., initial plan calculated on anatomy of the day). Ninety-five fractions were available for analysis, due to one patient not completing treatment. Table 2 quantifies the frequency of violations from the OAR constraints (Table A2) and coverage reductions (for PTV and GTV $D_{95\%}/D_{Rx}$) from the initial plan, for all patient's fractions. Note that 22 of the 95 $MRgRT_{BH}$ fractions were not adapted due to predicted dose meeting constraints. In total, the CT-$IGRT_{BH}$ plans had a 71.8% frequency of indications for adaptation compared to $MRgRT_{BH}$ plans at 83.0%. However, the predicted frequency of $D_{95\%}$ coverage reductions was higher on initial CT-$IGRT_{BH}$ plans (27.3%) compared to predicted $MRgRT_{BH}$ (22.1%). Note that the $MRgRT_{BH}$ adaptive dose had more frequent coverage reductions (average 27.0%) than $MRgRT_{BH}$ predicted dose (22.1%) to prevent constraint violations to the luminal GI OARs (incidence 0%). The CT-$IGRT_{BH}$ predicted 44.5% OAR constraint violations, compared to $MRgRT_{BH}$ dose at 60.9%.

An example of the advantage of adaptation over the predicted CT-$IGRT_{BH}$ dose (Fig. 4A) and predicted $MRgRT_{BH}$ dose (Fig. 4B) versus the adaptive $MRgRT_{BH}$ dose (Fig. 4C) on the fractional MRI of the day is shown. The $D_{0.5cc}$ stomach constraint of 35 Gy was violated at 36 Gy (Fig. 4A) and 47 Gy (Fig. 4B) respectively, with a PTV $V_{100\%}$ of only 59% (Fig. 4A, 4B) for both. The adaptive $MRgRT_{BH}$ resulted in a PTV and GTV $V_{100\%}$ of 74% and 92%, while reducing the stomach and small bowel dose below constraints.

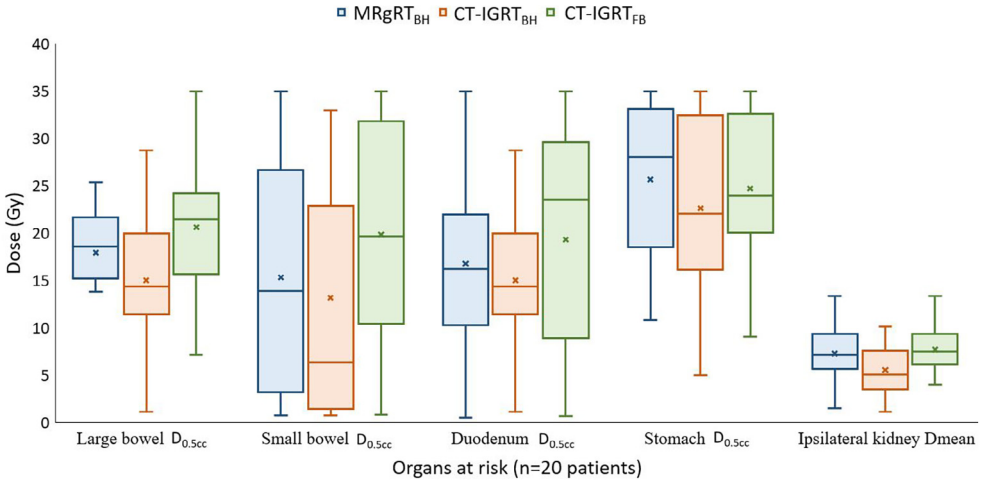

Fig. 2. Boxplot of the mean, median and interquartile ranges of maximum dose to 0.5 cc volumes for gastrointestinal organs at risk and mean dose to ipsilateral kidney for initial $MRgRT_{BH}$, ($n = 20$ plans), CT-$IGRT_{BH}$ ($n = 20$ plans), and CT-$IGRT_{FB}$ plans ($n = 20$ plans) for all 20 patients. Note that the median is denoted as horizontal line, the mean as an X, and outliers are not displayed. Note: Organ at risk (OAR), MR-guided radiotherapy with breath-hold ($MRgRT_{BH}$), CT based image-guided radiotherapy with breath-hold (CT-$IGRT_{BH}$), CT based image-guided radiotherapy with free-breathing (CT-$IGRT_{FB}$), dose to 0.5 cc volume ($D_{0.5cc}$), mean dose (D_{mean}), Gray (Gy).

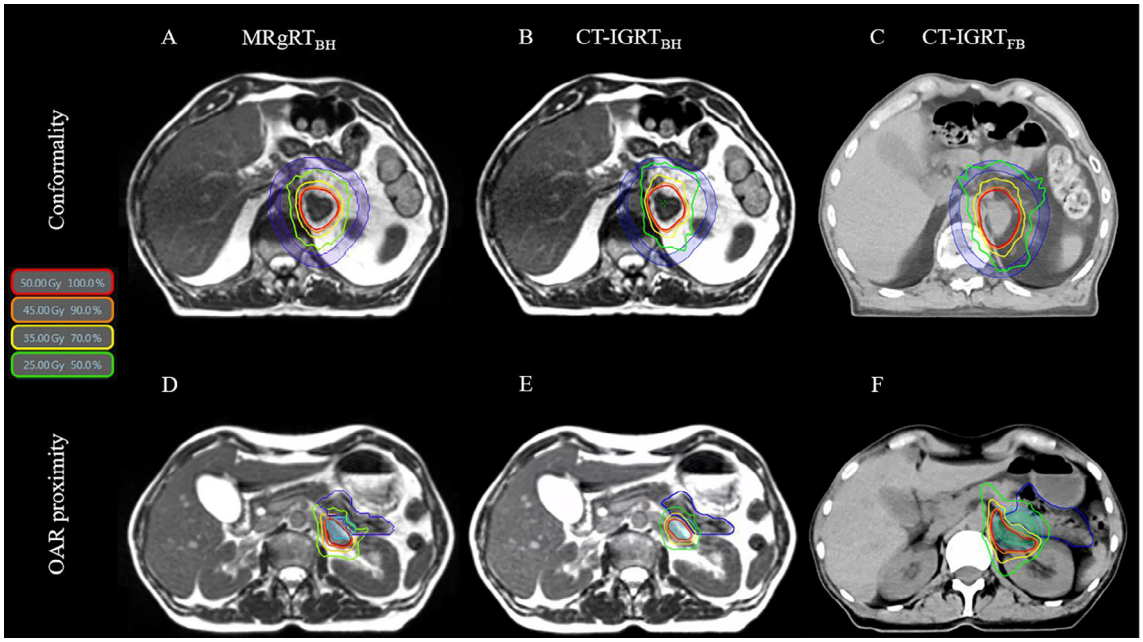

Fig. 3. Comparison of plan quality between MRgRT$_{BH}$ (A, D), CT-IGRT$_{BH}$ (B, E), and CT-IGRT$_{FB}$ (C, F) for two cases. The top row demonstrates the loss of low dose conformality in maximum dose to 2 cm (D_{2cm}) from the PTV surface due to the larger target size in free-breathing (C) compared to breath-hold (A, B). The bottom row shows increased overlap of the PTV (cyan) with the proximal small bowel (blue), due to the larger target size in free breathing (F) compared to breath hold (D, E) plans, demonstrating reduced target coverage in the CT-IGRT$_{FB}$ plan. Note: Organ at risk (OAR), MR-guided radiotherapy with breath-hold (MRgRT$_{BH}$), CT based image-guided radiotherapy with breath-hold (CT-IGRT$_{BH}$).

Discussion

To the best of our knowledge, this is the first report quantitatively evaluating the indication for adaptive breath-hold MR-guided radiotherapy compared to the standard treatment technique of CT-based image guided radiotherapy in the stereotactic ablation of adrenal malignancies. To this end, we investigated its impact on target volumes size and dosimetric qualities of coverage, conformality, and gastrointestinal luminal sparing.

Other studies have demonstrated BH compared to FB reduces the overall target volume and amount of irradiated normal tissues in thoracic and abdominal cancers. Gong *et al.* demonstrated a statistically significant 46% relative increase in PTV volume for esophageal cancers with FB versus deep inspiration breath hold (DIBH) as well as significant increases in dose to normal lung volumes [13]. Scotti *et al.* found similarly significant increases in PTV volume (23%) and normal lung volume doses for FB versus spirometer-controlled BH for lung cancer [14].

De Kuijer et al. evaluated the amount of superior to inferior adrenal motion with respiration through 4DCT to be 8.7 ± 4.2 mm for FB versus 2.4 ± 1.5 mm for Active Breathing Control (ABC) BH, although the overall margin was not statistically significant across 11 patients between the two techniques [8]. Our study, which applied a consistent 5 mm PTV expansion margin for all plans, did show a significant 71% increase ($p < 0.05$) in PTV volume for CT-IGRT$_{FB}$ over MRgRT$_{BH}$ techniques, due to the need for an ITV with FB. While de Kuijer et al. explored the overall motion envelope for adrenal metastases, the dosimetric difference due to the increase in PTV volume was not evaluated. Surprisingly, we also found a significant 9.6% decrease ($p < 0.01$) in median CT-IGRT$_{BH}$ PTV and GTV size compared to MRgRT$_{BH}$ which should have had exactly the same volumes.

The transfer of segmentation from ViewRay to Eclipse caused discrepancies due to masking of the ROI between the two software systems, so that partially filled voxels were truncated from all contours. This creates a limitation to our ability to compare the initial BH plan volumes, but possibly also the doses, as targets and OARs would be smaller and further apart on the CT-IGRT$_{BH}$ plans, which were approximated on the simulation MRIs. The contours on the daily fraction MRIs were also affected by segmentation difference upon being imported into Eclipse, resulting in potentially fewer OAR constraint violations in the CT-IGRT$_{BH}$ arm.

GTV coverage was significantly better ($p < 0.05$) for MRgRT$_{BH}$ than CT-IGRT$_{FB}$ at nearly all dose levels, possibly due to the significantly larger size of the ITV. The planning techniques for all plans in this study included a minimum relative dose of 120% to the gross disease with the hotspot driven to 130–140% of the prescription dose. Because increased ablative dose has been previously

Table 2
Indication for adaptation as evidenced by frequency of organ-at-risk violations and reductions in target coverage for the predicted CT-IGRT$_{BH}$ plans with respect to the predicted and adapted MRgRT$_{BH}$ plans. (n = 19 patients for 5 fractions).

Frequency of constraint violations			
OAR metric	CT-IGRT$_{BH}$ predicted dose	MRgRT$_{BH}$ predicted dose	MRgRT$_{BH}$ adaptive dose
Large Bowel ($D_{0.5\ cc}$)	4.4%	0%	0%
Small Bowel ($D_{0.5\ cc}$)	2.4%	4.7%	0%
Duodenum ($D_{0.5\ cc}$)	12.9%	14.3%	0%
Stomach ($D_{0.5\ cc}$)	18.9%	27.8%	0%
D_{mean} Kidney (ipsilateral)	5.9%	14.1%	0%
Total violations for subset of OAR constraints	44.5%	60.9%	0%
Frequency of coverage reductions from initial plan			
Target metric	CT-IGRT$_{BH}$ predicted dose	MRgRT$_{BH}$ predicted dose	MRgRT$_{BH}$ adaptive dose
PTV $D_{95\%}/D_{Rx}$	14.7%	5.3%	13.7%
GTV $D_{95\%}/D_{Rx}$	12.6%	16.8%	13.7%
Total coverage reductions	27.3%	22.1%	27.0%
Total indications for adaptation	71.8%	83.0%	N/A

Note: CT based image-guided radiotherapy with breath-hold (CT-IGRT$_{BH}$), MR-guided radiotherapy with breath-hold (MRgRT$_{BH}$), organ at risk (OAR), dose to 0.5 cc ($D_{0.5cc}$), mean dose (Dmean), dose to at least 95% of volume ($D_{95\%}$), prescription dose (D_{Rx})

shown to be favorable in terms of local control and overall survival in adrenal metastases [1], the difference in the amount of ablative dose coverage observed in this study is anticipated to translate into favorable clinical outcomes for adaptive $MRgRT_{BH}$, without increased risk to the OARs [1,17,18], but further investigation through prospective clinical trials is warranted.

In our study, the CT-$IGRT_{BH}$ plan demonstrated the advantage of VMAT over MRgRT IMRT plans in terms of target coverage, OAR sparing, homogeneity and of course $R_{50\%}$ gradient. This advantage was largely lost in the CT-$IGRT_{FB}$ plans, which exhibited a significant increase in dose to the small bowel, significant decreases in mean PTV and most GTV coverage metrics, and a loss in homogeneity, due to the large ITV. Interestingly, the $R_{50\%}$ gradient and the PITV are both significantly better, but both metrics are found by dividing by the very large ITV volume. Hoffman *et al.*, in a retrospective analysis of 277 protocol-acceptable SBRT lung plans, showed a predictable inverse relationship between the value of $R_{50\%}$ and the volume of the PTV for volumes less than 85 cc [19]. This was supported by Desai et al., who derived an analytical expression to calculate the theoretical minimum values of $R_{50\%}$ with a knowledge of the radius and surface area of the PTV [20]. Hoffman et al. and Desai et al. predict a lower theoretical $R_{50\%}$ value for the larger PTV volumes (median 91.9 cc) in CT-$IGRT_{FB}$, due to the need for an ITV, than for the smaller PTVs (53.6 cc) in $MRgRT_{BH}$. The Desai model assumes a spherical PTV, which was not evaluated for our study.

An advantage of MRgRT over CT-IGRT is that MR-guidance enables real-time tumor tracking and gating for each BH maneuver up to eight frames per second during the treatment delivery. For CT-$IGRT_{FB}$, treatment planning is reliant on a single respiratory cycle acquired during 4DCT simulation which may not be representative of the respiratory motion at the time setup and delivery [8,15] and CT-$IGRT_{BH}$ relies on a snapshot of the patient's anatomy at the time of simulation. While surrogate-based and/or fiducial tracking can be employed on CT-$IGRT_{BH}$ based planning and guidance, a larger overall uncertainty in the correlation to the adrenal tumor would be associated with this technique versus $MRgRT_{BH}$ [21] and Chen et al. has shown that BH techniques are not standard for CT-IGRT [1]. For soft tissue targets in the abdomen, it is routine clinical practice to obtain at least two confirmatory breath hold scans to calculate the CT-$IGRT_{BH}$ ITV. Such an approach was not accounted for in this study, and therefore our results underestimate the target volume and overestimate plan quality for the CT-$IGRT_{BH}$ technique. Continuous intrafraction motion management could be carried out in CT-based technologies, however limited reporting for adrenal BH studies on CT-IGRT have been demonstrated (i.e., 3 of 28 studies in a recent review published last year by Chen et al.) [1,2,3,22].

Respiratory-gated treatments also increase treatment time. Our results showed a 50% relative reduction in the total fractional treatment time with non-gated VMAT. The increase in treatment time for $MRgRT_{BH}$ includes delays due to respiratory or breath hold maneuver changes, in addition to delays due to internal anatomical changes potentially requiring 3D volumetric re-imaging and repositioning. CT-IGRT systems are unlikely to detect internal changes and could risk delivering ablative doses to sensitive OARs.

As has been previously published, online adaptive radiotherapy is known to reduce OAR doses and improve target coverage [6]. Our results for the $MRgRT_{BH}$ arm are consistent with previous findings. Without adaptation, the GI OARs would have received higher than prescribed doses as demonstrated by the 60.9% OAR violations for the predicted $MRgRT_{BH}$ dose. Of note is that the CT-$IGRT_{BH}$ demonstrated marginally fewer OAR violations (44.5%) on the anatomy of the day, due to the steeper gradient for VMAT over step-and-shoot IMRT. The more frequent coverage reductions for the CT-$IGRT_{BH}$ plans is a result of the lack of robustness to the target deformations within steep and conformal dose gradients of VMAT. The high frequency (71.8%) of indication for adaptation for the CT-$IGRT_{BH}$ arm is likely to have been undetected without daily soft tissue imaging. Greater frequencies in the indication for adaptation in each arm would have resulted from including all OAR constraints (Table A2) for each patient, however the heterogeneous requirements of the clinical trials involved made this effort prohibitive. It is uncertain to what extent the use of bulk densities affected the frequency of the indication for adaptation in the CT-$IGRT_{BH}$ arm.

A further limitation of our study is that 4DCT was performed without any abdominal compression. Therefore our values for

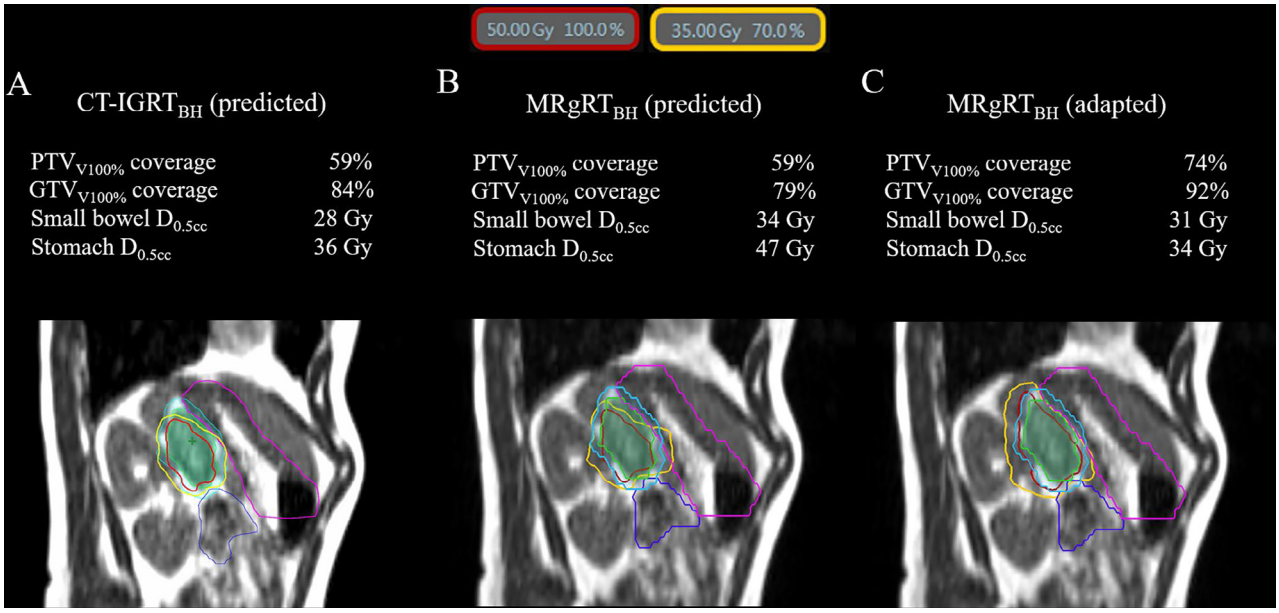

Fig. 4. Example of the indication for online adaptation quantified by recalculating the initial plan on the anatomy of the day, displayed for CT-$IGRT_{BH}$ (A) and $MRgRT_{BH}$ (B) for a single treatment fraction, in addition to the clinical online adaptive $MRgRT_{BH}$ plan (C) created and delivered for this fraction. Note: CT based image-guided radiotherapy with breath-hold (CT-$IGRT_{BH}$), MR-guided radiotherapy with breath-hold ($MRgRT_{BH}$), relative volume of the target covered by 100% of the prescription dose (V100%), maximum dose to 0.5 cc of the organ-at-risk (D0.05 cc), Gray (Gy).

ITV may be overestimated. Another potential limitation of this work is the retrospective nature of segmentation and treatment planning. Any inter-observer variability was minimized through peer review and editing of segmentation by two radiation oncologists. All CT-IGRT$_{FB}$ plans were reviewed for clinical acceptability by a medical physicist and radiation oncologist.

Another limitation of this study is the clinical impact of our results. The amount of normal tissue sparing for breath-hold was statistically significant compared to CT-IGRT$_{FB.}$ The VMAT CT-IGRT$_{BH}$ plan shows significantly better coverage and homogeneity than the IMRT MRgRT$_{BH}$ plans. And adaptive MRgRT can treat with far fewer OAR constraint violations, but the translation into clinical outcomes at this time is unknown. Future work will be required to assess the clinical local control and toxicity between the two approaches.

While two treating prescriptions were utilized in this study (e.g., 40 Gy and 50 Gy), the majority of patients were treated at 50 Gy (i.e., 70%). The analysis performed enabled independence of prescription (i.e., coverage normalized to respective prescription). The amount of irradiated normal tissues was found to be dependent on the size of the treatment volume (i.e., free breathing vs breath hold) and technique (i.e., IMRT vs VMAT) with minor contributions from the overall prescription. If a patient was planned for 40 Gy on the MRgRT$_{BH}$ course, then the same parameters of target coverage goals and OARs were utilized for CT-IGRT$_{BH}$ and CT-IGRT$_{FB}$.

The results of this study may in fact overestimate the amount of coverage clinically achievable in CT-IGRT for FB or BH. The CT-IGRT target coverage was artificially higher than clinically acceptable, due to the fact that the same GI PRV was utilized in all arms. In reality, the spatial gradient within overlapping GI PRV to PTV would need to be more conservatively positioned for actual clinical CT-IGRT, since daily online adaptive radiotherapy would not be available on the c-arm platform. Our approach of using the same GI PRV was only to investigate the dosimetric differences due to the ITV versus BH approach and the BH VMAT vs IMRT techniques, irrespective of online adaptive versus conventional delivery techniques. Online adaptive radiotherapy was used for all adrenal MRgRT$_{BH}$ treatments due to the aforementioned ablative doses in proximity to GI OARs.

In conclusion, initial plans for VMAT CT-IGRT$_{BH}$ were shown to be dosimetrically superior in target coverage, conformality, and OAR sparing to the large bowel, duodenum, and ipsilateral kidney versus IMRT MRgRT$_{BH}$. However, the majority of fractions had OAR constraint violations when the initial CT-IGRT$_{BH}$ plans were calculated on the anatomy of the day. MR-guided adaptive radiotherapy enabled no OAR violations to the luminal GI organs. The highly conformal CT-IGRT$_{BH}$ plans were less robust to interfractional target changes, compared to MRgRT$_{BH}$ coverage. The dosimetric advantages of VMAT were lost when applied to the standard free breathing ITV-approach of CT-based IGRT. Compared to CT-IGRT$_{FB}$, MRgRT$_{BH}$ enabled significant reductions in target volumes, marginally improved PTV coverage, and significant improvements in GTV coverage and small bowel sparing.

Conflict of interest statements

- Ms. Rodriguez has grant support for this work from ViewRay Inc.
- Dr. Kotecha reports honoraria from Accuray Inc., Elekta AB, ViewRay Inc., Novocure Inc., Elsevier Inc. and institutional research funding from Medtronic Inc., Blue Earth Diagnostics Ltd., Novocure Inc., GT Medical Technologies, AstraZeneca, Exelixis, and ViewRay Inc.
- Dr. Tom reports research funding from Blue Earth Diagnostics.
- Dr. Chuong reports personal fees from ViewRay Inc., Sirtex, Advanced Accelerator Applications, and grants from ViewRay Inc., AstraZeneca, Novocure, outside the submitted work.
- Dr. Contreras has nothing to disclose.
- Dr. Romaguera has nothing to disclose.
- Ms. Alvarez has nothing to disclose.
- Dr. McCulloch has nothing to disclose.
- Mr. Herrera has nothing to disclose.
- Mr. Hernandez has nothing to disclose.
- Mr. Mercado has nothing to disclose.
- Dr. Mehta reports personal fees from Zap, Mevion, Karyopharm, Tocagen, AstraZeneca; and from BOD Oncoceutics.
- Dr. Gutierrez reports personal fees from Elekta and ViewRay, Inc.
- Dr. Mittauer reports personal fees from ViewRay Inc., other from MR Guidance LLC, and grants from ViewRay Inc.

Funding support

This research was supported by grant funding from ViewRay Inc.

Data availability

Research data are not available at this time.

Appendix A

Table A1
Patient and tumor characteristics

Characteristic		*N* (Range)
Number of patients		20
Median age in years at adrenal treatment		60 (27–75)
Sex		
	Male	10
	Female	10
ECOG performance status		
	0	2
	1	15
	2	2
	3	1
Laterality		
	Left	11
	Right	9
Primary Tumor type		
	Bladder	1
	Breast	1
	Esophagus	1
	Lung	17
Histology		
	Adenocarcinoma	13
	Adenosquamous NSCC	1
	Angiosarcoma	1
	Infiltrating Ductal Carcinoma	1
	Squamous Cell Carcinoma	1
	Small Cell Carcinoma	2
	Urothelial Carcinoma	1
AJCC stage at primary diagnosis		
	IA	1
	IB	2
	IIA	0
	IIB	1
	III	2
	IIIA	1
	IIIB	3
	IIIC	1
	IV	9
AJCC stage at adrenal treatment		
	IV	20
Prescribed dose		
	Median (Range) in Gy	50 (40–50)
Fractions		5

Note: number (N), Eastern Cooperative Oncology Group (ECOG), Non-small cell carcinoma (NSCC), American Joint Committee on Cancer (AJCC), Gray (Gy)

Table A2
Overview of OAR constraints for patients in this study (n = 20 patients × 5 fractions).

Organ at risk	Metric	Median	Range		
Esophagus	$D_{0.03cc}$	35	30	–	35
	D_{5cc}	27.5	27.5	–	27.5
Stomach	$D_{0.03cc}$	39	33	–	40
	$D_{0.5cc}$	35	33	–	35
	D_{5cc}	26.5	26.5	–	26.5
Duodenum	$D_{0.03cc}$	38	34.5	–	40
	$D_{0.5cc}$	33	30	–	35
Large Bowel	$D_{0.03cc}$	35	25	–	43
	$D_{0.5cc}$	33	30	–	38
	D_{30cc}	24	24	–	24
Small Bowel	$D_{0.03cc}$	36.5	34.5	–	40
	$D_{0.5cc}$	33	30	–	35
	D_{30cc}	24	24	–	24
Kidneys	D_{200cc}	17.5	17.5	–	17.5
	D_{mean} (Ipsilateral)	8	5	–	10
	D_{mean} (Contralateral)	6	3	–	10
Spinal Canal	$D_{0.03cc}$	28	20	–	45
	$D_{0.35cc}$	22	22	–	22
	$D_{1.2cc}$	15.5	15.5	–	15.5
Liver	D_{700cc}	21	21	–	21
	D_{mean}	13	10	–	18
Skin	$D_{0.03cc}$	38.5	38.5	–	38.5
	D_{10cc}	36.5	36.5	–	36.5

Note: Organ at risk (OAR), dose to 0.03 cc volume ($D_{0.03cc}$), dose to 5 cc (D_{5cc}), dose to 0.5 cc ($D_{0.5cc}$), dose to 30 cc (D_{30cc}), dose to 200 cc (D_{200cc}), mean dose (D_{mean}), dose to 0.35 cc ($D_{0.35cc}$), dose to 1.2 cc ($D_{1.2cc}$), dose to 700 cc (D_{700cc}), dose to 10 cc (D_{10cc})

References

[1] Chen WC, Baal JD, Baal U, Pai J, Gottschalk A, Boreta L, et al. Stereotactic Body Radiation Therapy of Adrenal Metastases: A Pooled Meta-Analysis and Systematic Review of 39 Studies with 1006 Patients. Int J Radiat Oncol Biol Phys 2020;107:48–61. https://doi.org/10.1016/j.ijrobp.2020.01.017.

[2] Oshiro Y, Takeda Y, Hirano S, Ito H, Aruga T. Role of radiotherapy for local control of asymptomatic adrenal metastasis from lung cancer. Am J Clin Oncol 2011;34:249–53. https://doi.org/10.1097/COC.0b013e3181dbb727.

[3] Buergy D, Rabe L, Siebenlist K, et al. Treatment of adrenal metastases with conventional or hypofractionated image-guided radiation therapy - patterns and outcomes. Anticancer Res 2018;38(8):4789–96. https://doi.org/10.21873/anticanres.12788.

[4] König L, Häfner MF, Katayama S, Koerber SA, Tonndorf-Martini E, Bernhardt D, et al. Stereotactic body radiotherapy (SBRT) for adrenal metastases of oligometastatic or oligoprogressive tumor patients. Radiat Oncol 2020;15. https://doi.org/10.1186/s13014-020-1480-0.

[5] Chance WW, Nguyen Q-N, Mehran R, Welsh JW, Gomez DR, Balter P, et al. Stereotactic ablative radiotherapy for adrenal gland metastases: factors influencing outcomes, patterns of failure, and dosimetric thresholds for toxicity. Pract Radiat Oncol 2017;7:e195–203. https://doi.org/10.1016/j.prro.2016.09.005.

[6] Palacios MA, Bohoudi O, Bruynzeel AME, van Sörsen de Koste JR, Cobussen P, Slotman BJ, et al. Role of daily plan adaptation in MR-guided stereotactic ablative radiation therapy for adrenal metastases. Int J Radiat Oncol Biol Phys 2018;102:426–33. https://doi.org/10.1016/j.ijrobp.2018.06.002.

[7] Lee J, Dean C, Patel R, Webster G, Eaton DJ. Multi-center evaluation of dose conformity in stereotactic body radiotherapy. Phys Imaging Radiat Oncol. 2019;11:41-46. Published 2019 Aug 28. 10.1016/j.phro.2019.08.002

[8] de Kuijer M, van Egmond J, Kouwenhoven E, Bruijn-Krist D, Ceha H, Mast M. Breath-hold versus mid-ventilation in SBRT of adrenal metastases. Tech Innov Patient Support Radiat Oncol. 2019;12:23-27. Published 2019 Dec 16. 10.1016/j.tipsro.2019.11.007.

[9] Mittauer K, Paliwal B, Hill P, et al. A new era of image guidance with magnetic resonance-guided radiation therapy for abdominal and thoracic malignancies. Cureus. 2018;10(4):e2422. Published 2018 Apr 4. 10.7759/cureus.2422.

[10] Botticella A, Levy A, Auzac G, Chabert I, Berthold C, Le Pechoux C. Tumour motion management in lung cancer: a narrative review. Transl Lung Cancer Res 2021;10:2011–7. https://doi.org/10.21037/tlcr10.21037/tlcr-20-856.

[11] Keall PJ, Mageras GS, Balter JM, et al. The management of respiratory motion in radiation oncology report of AAPM Task Group 76. Med Phys 2006;33:3874–900. https://doi.org/10.1118/1.2349696.

[12] Henke L, Kashani R, Robinson C, Curcuru A, DeWees T, Bradley J, et al. Phase I trial of stereotactic MR-guided online adaptive radiation therapy (SMART) for the treatment of oligometastatic or unresectable primary malignancies of the abdomen. Radiother Oncol 2018;126:519–26. https://doi.org/10.1016/j.radonc.2017.11.032.

[13] Gong G, Wang R, Guo Y, et al. Reduced lung dose during radiotherapy for thoracic esophageal carcinoma: VMAT combined with active breathing control for moderate DIBH. Radiat Oncol. 2013;8:291. Published 2013 Dec 20. 10.1186/1748-717X-8-291.

[14] Scotti V, Marrazzo L, Saieva C, Agresti B, Meattini I, Desideri I, et al. Impact of a breathing-control system on target margins and normal-tissue sparing in the treatment of lung cancer: experience at the radiotherapy unit of Florence University. Radiol Med 2014;119:13–9. https://doi.org/10.1007/s11547-013-0307-6.

[15] Lens E, van der Horst A, Kroon PS, van Hooft JE, Dávila Fajardo R, Fockens P, et al. Differences in respiratory-induced pancreatic tumor motion between 4D treatment planning CT and daily cone beam CT, measured using intratumoral fiducials. Acta Oncol 2014;53:1257–64. https://doi.org/10.3109/0284186X.2014.905699.

[16] Mittauer KE, Hill PM, Bassetti MF, Bayouth JE. Validation of an MR-guided online adaptive radiotherapy (MRgoART) program: deformation accuracy in a heterogeneous, deformable, anthropomorphic phantom. Radiother Oncol 2020;146:97–109. https://doi.org/10.1016/j.radonc.2020.02.012.

[17] Arcidiacono F, Aristei C, Marchionni A, et al. Stereotactic body radiotherapy for adrenal oligometastasis in lung cancer patients. Br J Radiol 2020;93:20200645. https://doi.org/10.1259/bjr.20200645.

[18] Chuong MD, Bryant J, Mittauer KE, et al. Ablative 5-fraction stereotactic magnetic resonance-guided radiation therapy with on-table adaptive replanning and elective nodal irradiation for inoperable pancreas cancer [Published correction appears in Pract Radiat Oncol. 2021 May-Jun;11(3):e354]. Pract Radiat Oncol. 2021;11:134-147. 10.1016/j.prro.2020.09.005.

[19] Hoffman D, Dragojević I, Hoisak J, Hoopes D, Manger R. Lung Stereotactic Body Radiation Therapy (SBRT) dose gradient and PTV volume: a retrospective multi-center analysis. Radiat Oncol. 2019;14:162. Published 2019 Sep 3. 10.1186/s13014-019-1334-9.

[20] Desai DD, Johnson EL, Cordrey IL. An analytical expression for $R_{50\%}$ dependent on PTV surface area and volume: a lung SBRT comparison. J Appl Clin Med Phys 2020;21:278–82. https://doi.org/10.1002/acm2.v21.1110.1002/acm2.13026.

[21] Wang J, Li F, Dong Y, Song Y, Yuan Z. Clinical study on the influence of motion and other factors on stereotactic radiotherapy in the treatment of adrenal gland tumor. Onco Targets Ther. 2016;9:4295-4299. Published 2016 Jul 15. 10.2147/OTT.S107106.

[22] Chawla S, Chen Y, Katz AW, Muhs AG, Philip A, Okunieff P, et al. Stereotactic body radiotherapy for treatment of adrenal metastases. Int J Radiat Oncol Biol Phys 2009;75:71–5. https://doi.org/10.1016/j.ijrobp.2008.10.079.